0026-895X/04/6504-868–879$20.00
MOLECULAR PHARMACOLOGY
Copyright © 2004 The American Society for Pharmacology and Experimental Therapeutics
Mol Pharmacol 65:868–879, 2004

Vol. 65, No. 4
2983/1140113
Printed in U.S.A.

Potent Cyclic Antagonists of the Complement C5a Receptor on Human Polymorphonuclear Leukocytes. Relationships between Structures and Activity

Darren R. March, Lavinia M. Proctor, Martin J. Stoermer, Robert Sbaglia, Giovanni Abbenante, Robert C. Reid, Trent M. Woodruff, Khemar Wadi, Natalii Paczkowski, Joel D. A. Tyndall, Stephen M. Taylor, and David P. Fairlie

Institute for Molecular Bioscience (D.R.M., M.J.S., R.S., G.A., R.C.R., J.D.A.T., D.P.F.) and School of Biomedical Sciences (L.M.P., T.M.W., K.W., N.P., S.M.T.), University of Queensland, Brisbane, Queensland, Australia

Received September 22, 2003; accepted January 7, 2004

This article is available online at http://molpharm.aspetjournals.org

ABSTRACT

Human C5a is a plasma protein with potent chemoattractant and pro-inflammatory properties, and its overexpression correlates with severity of inflammatory diseases. C5a binds to its G protein-coupled receptor (C5aR) on polymorphonuclear leukocytes (PMNLs) through a high-affinity helical bundle and a low-affinity C terminus, the latter being solely responsible for receptor activation. Potent and selective C5a antagonists are predicted to be effective anti-inflammatory drugs, but no pharmacophore for small molecule antagonists has yet been developed, and it would significantly aid drug design. We have hypothesized that a turn conformation is important for activity of the C terminus of C5a and herein report small cyclic peptides that are stable turn mimics with potent antagonism at C5aR on human PMNLs. A comparison of solution structures for the C terminus of C5a, small acyclic peptide ligands, and cyclic antagonists supports the importance of a turn for receptor binding. Competition between a cyclic antagonist and either C5a or an acyclic agonist for C5aR on PMNLs supports a common or overlapping binding site on the C5aR. Structure-activity relationships for 60 cyclic analogs were evaluated by competitive radioligand binding with C5a (affinity) and myeloperoxidase release (antagonist potency) from human PMNLs, with 20 compounds having high antagonist potencies (IC_{50}, 20 nM-1 μM). Computer modeling comparisons reveal that potent antagonists share a common cyclic backbone shape, with affinity-determining side chains of defined volume projecting from the cyclic scaffold. These results define a new pharmacophore for C5a antagonist development and advance our understanding of ligand recognition and receptor activation of this G protein-coupled receptor.

Activation of the complement system, a cascading network of plasma proteins, is crucial in host defense to infection and injury (Abbas et al., 1997). The ultimate product of complement activation is the membrane attack complex that is responsible for bacterial cell lysis. Along the way, 70- to 80-residue pro-inflammatory anaphylatoxins C3a, C4a, and C5a are also produced. C5a is a very potent pro-inflammatory agent that interacts with a G protein-coupled C5a receptor (C5aR) on the surface of myeloid (e.g., neutrophils, eosinophils, monocytes, T lymphocytes, and macrophages) and non-myeloid cells (e.g., vascular endothelial cells, vascular smooth muscle, neurons, glial cells, astrocytes, and mast cells) (Wetsel, 1995; Zwirner et al., 1999; Barnum, 2002). C5a is a potent chemotaxin for inflammatory cells and causes smooth muscle spasmogenesis as well as release of lysozomal enzymes, reactive oxygen species, and inflammatory cytokines (e.g., TNF-α, IL-1, -6, -8) (Okusawa et al., 1988; Ember et al., 1994, 1998), all components of the host response to injury or infection.

Sustained or aberrant complement activation is associated with tissue damage and inflammatory disease. Elevated levels of C5a correlate with immune and inflammatory conditions (Kohl, 2001) and there is growing evidence that C5a is pathogenic in numerous inflammatory diseases (Abbas et al., 1997; Kohl, 2001; Barnum, 2002), including rheumatoid ar-

This work was supported in part by the Australian National Health and Medical Research Council and the Australian Research Council.

D.R.M. and L.M.P. should be considered joint first authors.

ABBREVIATIONS: TNF-α, tumor necrosis factor-α; IL, interleukin; TFA, trifluoroacetic acid; DIEA, *N*,*N*-diisopropylethylamine; DMF, *N*,*N*-dimethylformamide; HBTU, 2-(1H-benzotriazol-1-yl)-1,1,3,3-tetramethyluronium hexafluorophosphate; rpHPLC, reversed-phase high-performance liquid chromatography; DMF, dimethylformamide; C5a, complement factor 5a; C5aR, C5a receptor; Boc, *N*-*tert*-butoxycarbonyl; Fmoc, fluoromethyloxycarbonyl; TOCSY, total correlation spectroscopy; ECOSY, exclusive correlation spectroscopy; NOESY, nuclear Overhauser effect (or enhancement) spectroscopy; 1D, one-dimensional; Cha, cyclohexylalanine; MPO, myeloperoxidase; PMNL, polymorphonuclear leukocyte.

thritis, immune complex disease, inflammatory bowel syndromes, ischemia/reperfusion injury, myocardial infarct, pancreatitis, cystic fibrosis, multiple sclerosis, atherosclerosis, fibrosis, allergy, diabetes type I, Alzheimer's disease, graft rejection, gingivitis, and psoriasis.

The binding site for C5a on its receptor and structural features of both receptor and ligands that influence agonism and antagonism are poorly defined. The solution structure of C5a (Zuiderweg et al., 1989; Zhang et al., 1997) consists of a 64-residue, high-affinity 'receptor-binding' N-terminal helix bundle attached to a 10-residue low affinity 'receptor-activating' C-terminal domain thought to bind in a transmembrane pore region of the receptor (Siciliano et al., 1994; Huber-Lang et al., 2003). Much effort has been devoted to developing short peptides derived from the C terminus of C5a as agonists/antagonists (Drapeau et al., 1993; Luly et al., 1993; Konteatis et al., 1994; Sanderson et al., 1994, 1995; Finch et al., 1997). Most were partial agonists, but the hexapeptide MeFKPdChaWr was a full antagonist with <1 μM affinity for the C5aR (Drapeau et al., 1993; Konteatis et al., 1994). More recently, we demonstrated that MeFKPdChaWr and other hexapeptides adopt a turn conformation in solution (Wong et al., 1998) and the cyclic molecule AcF-[OPdChaWR] (**1**) (Fig. 1) was a potent and selective antagonist of C5aR on human immune cells (Finch et al., 1999; Haynes et al., 2000) with potent anti-inflammatory activity in vivo (Short et al., 1999; Strachan et al., 2000, 2001; Arumugam et al., 2002, 2003; Woodruff et al., 2002, 2003).

Herein, we investigate structure-potency relationships for 60 cyclic antagonists like **1**, report solution structures that define cyclic backbone shape and side chain projections (through Cα-Cβ and Cβ-Cγ vectors) for three cyclic antagonists, and compare structures and receptor binding properties with C5a and small acyclic peptide ligands. This information reveals how the cyclic scaffold directs important side chains of Phe, dCha, Trp, and Arg in **1** for receptor binding and antagonism, information that is valuable for our understanding of the mechanism of antagonism, the activation of C5aR, for refining the antagonist pharmacophore and for developing potent and selective nonpeptidic C5aR antagonists into drugs.

Materials and Methods

Chemical Synthesis

General Methods. Protected amino acids and resins (Novabiochem, Laufelfingen, Switzerland), TFA, DIEA, and DMF (peptide synthesis grade; Auspep, Parkville, Victoria, Australia), HBTU and BOP (Richelieu Biotechnologies, St Hyacinthe, QC, Canada) were obtained from commercial sources. All other materials were reagent grade. Preparative scale reversed-phase HPLC (rpHPLC) separations were performed on a Vydac C18 column (2.2 × 25 cm); analytical rpHPLC on VYDAC or Phenomenex C18 column (250 × 4.6 mm); using gradient mixtures of solvent A = water/0.1% TFA and solvent B = water 10%/acetonitrile 90%, 0.09% TFA. The molecular weight was determined by electrospray mass spectrometry (LCT MICROMASS). All compounds were analyzed for purity and molecular weight by rpHPLC and mass spectrometry.

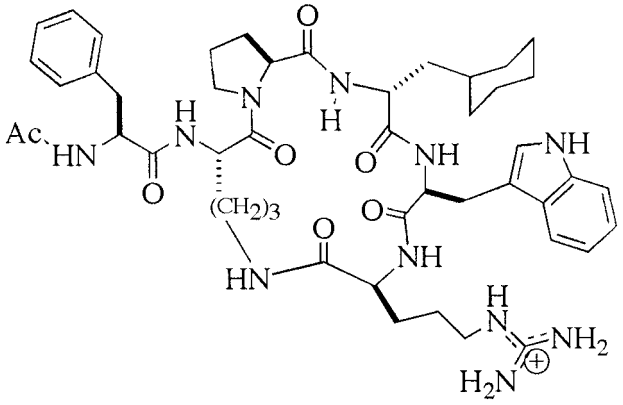

Fig. 1. Chemical structure of AcF-[OPdChaWR].

Peptide Synthesis. His6-tagged rhC5a was synthesized (Paczkowski et al., 1999) with incorporation of a tobacco etch virus (TEV) cleavage site between the His_6 tag and C5a, allowing tag removal with retention of an N-terminal tripeptide (GGS). AcF[^{3}H][OP[$^3H_2$]dChaWR] was synthesized (Multiple Peptide Systems, San Diego, CA) and purified to >99% by rpHPLC (25–70% B in 20 min). The specific activity was 60 Ci/mmol. Short peptides were assembled by manual step-wise solid phase peptide synthesis using Boc or Fmoc chemistry (Wong et al., 1998; Finch et al., 1999).

Cyclic Peptide Synthesis. In general, linear peptides (1 Eq) and BOP (5 Eq) were dissolved in DMF (10 mM peptide concentration) before adding DIEA (15 Eq) and stirred at room temperature overnight. DMF was removed in vacuo at 30°C and compounds purified by rpHPLC. For cyclic peptides containing a free N terminus, an Fmoc group was used as the N-terminal–protecting group during cyclization, after which the peptide was treated with 30% piperidine/DMF and worked up as above. One example is given below for each Boc and Fmoc syntheses of cyclic compounds, together with characterization by mass spectrometry and rpHPLC retention times (Rt; in minutes) under specified elution conditions.

Synthesis of Cycle AcF-[OPdChaWR] (1). The peptide Ac-Phe-Orn-Pro-dCha-Trp-Arg was synthesized by Boc chemistry on a 0.20-mmol scale using HBTU/DIEA activation and in situ neutralization on a Boc-L-Arg(Tos)-phenylacetamidomethyl] resin (338 mg, substitution value = 0.591 mmol/g). Cleavage and deprotection of the resin (457 mg) was achieved by treating the resin with HF (10 ml) and *p*-cresol (1 ml) at −5 to 0°C for 1 to 2 h, to give crude peptide (160 mg, 90%). Cyclization involved stirring the crude peptide (41 mg, 45 μmol), BOP (126 mg, 0.28 mmol), and DIEA (158 μl, 0.9 mmol) in DMF (57 ml) for 15 h. Solvent was removed in vacuo, and the cyclic peptide was purified by rpHPLC (18.8 mg, 47%) Rt = 10.8 min (gradient, 70% A/30% B to 0% A/100% B over 30 min). Mass spectrometry: [M+H]+ (calc.) = 896.5, (found) = 896.5.

Synthesis of cycle AcF-[OPdCha(*N*-Me-Phe)R] (43). Linear peptide Ac-Phe-Orn-Pro-dCha-(*N*-Me-Phe)-Arg-OH was synthesized by Fmoc chemistry using HBTU/DIEA activation and in situ neutralization on Fmoc-L-Arg(pbf)-Wang resin (0.35 mmol/g; Novabiochem) using Fmoc-*N*-methyl-L-Phe-OH (281 mg, 2 Eq), Fmoc-dCha (275 mg, 2 Eq), Fmoc-Pro (472 mg, 4 Eq), Fmoc-Orn(Boc) (477 mg, 3 Eq), Fmoc-Phe (542 mg, 4 Eq), and Ac_2O (4 Eq). Cleavage and deprotection of resin with 95% TFA (15 ml) for 1 h gave crude peptide (150 mg) after precipitation with diethyl ether. Cyclization involved stirring the rpHPLC purified peptide (100 mg), BOP (200 mg), and DIEA (222 μl) in DMF (2 ml) for 4 h. Solvent was removed in vacuo and cyclic peptide was purified by rpHPLC (50 mg) Rt = 33 min (gradient: 70% A/30% B to 0% A/100% B over 30 min). Mass spectrometry: [M+H]+ (calc.) = 871.5, (found) = 871.5.

Structural Analysis

NMR Spectra. ^{1}H NMR spectra were recorded on 4 mM peptides in DMSO-d_6 (550 μl) on Bruker ARX 500 and Avance DRX 500 spectrometers at 293, 298, and 308 K. Proton assignments were made by TOCSY (80 ms mixing time), double quantum-filtered correlation spectroscopy, ECOSY, and NOESY (40-, 120-, and 350-ms mixing time) spectra using a sequential assignment method (Wuthrich, 1986). Variable-temperature 1D ^{1}H and TOCSY spectra were typically collected at 5-K increments from 293 to 338 K. For identi-

fication of slowly exchanging amides, a series of 1D and TOCSY spectra were run after diluting samples with D_2O (100 μl).

Structure Calculations. Backbone dihedral angle restraints were derived from $^3J_{H,NH}$ coupling constants measured from high-resolution 1D ^{1}H NMR spectra; angles were restrained to $-120° \pm 30$ for $^3J_{H\alpha,NH} > 8.2$ Hz and to $-60° \pm 20$ for $^3J_{H\alpha,NH} < 5$ Hz ($+60° \pm 20$ for $^3J_{H\alpha,NH} < 5$ Hz for D-amino acids). Stereospecific assignments of β-methylene protons and χ-1 dihedral angles were determined by examining $^3J_{H}\alpha$,Hβ coupling constants in high-resolution 1D ^{1}H NMR and ECOSY spectra in combination with NOE peak intensities at short mixing times (40, 120 ms). No explicit hydrogen bonds were used as distance restraints in structure calculations. NOE distance restraints were derived from spectra at 308 K, but lower temperature NOESY spectra were also used to resolve ambiguities arising from aromatic NH overlap.

Solution structures were calculated using simulated annealing and energy minimization protocols within XPLOR 3.851 (Brünger, 1992). Standard topology and parameter files for Lys were modified to accommodate ornithine, and an amide bond patch connected the Arg C terminus to the ornithine side chain. Cyclohexylalanine (Cha)-containing peptides were modeled as Leu, as Cha parameters within topallhdg5.2.pro and parallhdg5.2.pro gave consistently high >10° dihedral and violations. Initial structures were generated using random Φ,ψ dihedral angles and energy-minimized. Preliminary structures were generated by torsion angle simulated annealing involving a high-temperature (50,000 K) phase comprising 1000 steps of 0.015 ps of torsion angle dynamics, a cooling phase with 1000 steps of 0.015 ps of torsion angle dynamics during which the temperature was lowered to 0 K, and an energy minimization phase comprising 2000 steps of Powell minimization. Typically, 50 structures were calculated and the 20 structures of lowest energy were superimposed and compared using InsightII and Promotif.

Cellular Assays

Polymorphonuclear Leukocytes. Human PMNLs were isolated from heparinized whole blood by density gradient separation over a Ficoll-Hypaque solution (Histopaque 1077; Sigma, St. Louis, MO) as described previously (Finch et al., 1999).

Receptor Binding Assay. PMNLs (2×10^5) or PMNL membranes (0.5–1 μg protein) were incubated (4°C, 60 min) in a 96-well multiscreen filtration plate (GV 0.22 μM; Millipore, North Ryde, New South Wales, Australia) with buffer (50 mM HEPES, 1 mM $CaCl_2$, 5 mM $MgCl_2$, 0.5% bovine serum albumin, and 0.1% bacitracin), ^{125}I-C5a (50 pM; PerkinElmer Life and Analytical Sciences, Boston, MA) or [$^3H_3$]AcF-[OPdChaWR] (830 pM; Multiple Peptide Systems) and test compound to a total volume of 200 μl. The wells were then filtered, dried, and the filter-bound radioactivity was counted. Nonspecific binding was assessed by the addition of 100 nM C5a, which typically resulted in 5 to 10% total binding for intact PMNLs and 10 to 20% for PMNL membranes.

Myeloperoxidase Release. PMNLs (1×10^5) were preincubated (10 min, 37°C) with cytochalasin B (10 μg/ml; Sigma) before being added to a 96-well plate containing buffer (Hanks' buffered salt solution + 0.1% gelatin) and test compounds, as described previously (Paczkowski et al., 1999). The plate was incubated (10 min, 37°C), C5a was added (MPO release assigned as 100% response), and the plate was incubated again (10 min, 37°C). The total final reaction volume was 125 μl. Phosphate buffer, pH 6.8, was added to each well, a final incubation was performed (10 min, 25°C), and was substrate added (3,3-dimethoxybenzidine; 2.85 mg/ml; Sigma) + H_2O_2 (0.255%; Merck). The absorbance of each well was read at 450 nm on a TECAN microplate reader, with maximal C5a-induced MPO release assigned 100% response versus spontaneous MPO release ~5% (subtracted from all values).

Statistical Analysis. Dissociation constants (K_b) for the antagonist were measured as detailed elsewhere (Kenakin, 1997; Paczkowski et al., 1999). For both receptor binding and antagonism assays, nonlinear regression was performed using Prism 3 (GraphPad Software, San Diego, CA), inhibition curves were produced, and IC_{50} values were determined. Receptor affinities and antagonist potencies ($-\log IC_{50}$) were compared statistically with compound **1** using a one-way analysis of variance coupled with a Tukey post test, and statistical significance was determined ($P \leq 0.05$).

Results

Competitive Binding/Antagonism

Compound **1** is a potent antagonist of the human C5aR as measured by inhibition of the release of myeloperoxidase from human PMNLs, activated by either human recombinant C5a (Fig. 2A) or a small agonist (Finch et al., 1997) peptide analog YSFKPMPLaR of the C terminus of C5a (Fig. 2B). Moreover, [^{3}H]Compound **1**, which has an affinity of 21 nM ($-\log IC_{50} = 7.68 \pm 0.01$, $n = 3$), competes with an acyclic peptide antagonist, MeFKPdChaWr (IC_{50} = 201 nM, $-\log IC_{50} = 6.70 \pm 0.06$, $n = 3$), and YSFKPMPLaR (IC_{50} = 1180 nM, $-\log IC_{50} = 5.93 \pm 0.15$, $n = 4$) for binding to human PMNL C5aRs (Fig. 2C). Importantly, Fig. 2 suggests that the binding of antagonist **1**, agonist YSFPMPLaR, antagonist MeFKPdChaWr and C5a may occur at the same or overlapping sites on the C5aR. This is supported below by the finding of a common structural turn motif in all four compounds. Compound **1** has an apparent receptor affinity of 48 nM to human PMNL membranes, with a K_b of 1 nM ($pK_b = 9.00 \pm 0.04$, $n = 3$) or 9 nM ($pK_b = 8.04 \pm 0.35$, $n = 3$) against MPO release from human PMNLs induced by YSFKPMPLaR or recombinant C5a, respectively (Fig. 2). By comparison, the acyclic peptide antagonist MeFKPdChaWr has an apparent receptor affinity for human PMNL membranes of 370 nM and K_b of 51 nM against C5a-induced myeloperoxidase release from human PMNLs (Paczkowski et al., 1999). The superior receptor affinity and antagonist potency of **1** versus 'linear' peptide antagonists such as MeFKPdChaWr is attributed to preorganization of the constrained cycle in **1** to the same or similar putative receptor-binding shape adopted naturally by the C terminus of C5a (Fig. 4B). Energy is needed for solution structures to reorganize to the optimal shape recognized by a receptor, and an unfavorable position of this equilibrium leads to low receptor affinity and modest potency of unconstrained peptides. Elsewhere, we demonstrate that antagonism exhibited by **1** is insurmountable (Paczkowski et al., 1999), reflecting a slow off rate from the receptor.

Structure of AcF-[OPdChaWR] (1)

We have reported a preliminary solution structure for the backbone of **1** (Finch et al., 1999) that did not define side-chain locations and used inferior topology and parameter files to those now available for structure calculations. In this structural refinement of **1**, positions for Orn, Pro, Trp, Phe side chains are now defined, the latter two by using χ_1 dihedral restraints. These modifications more accurately define macrocycle shape and locations of side chains responsible for affinity and antagonism. Importantly, the structure of **1** was determined under the same conditions as structures of other cycles herein, allowing direct structural comparisons.

Coupling Constants and Temperature-Independent Chemical Shifts. ^{1}H NMR spectra and resonance assignments were similar to those previously reported (Finch et al., 1999), suggesting structure around Phe2, D-Cha5, and Arg7. In addition to three ψ angle restraints derived from coupling

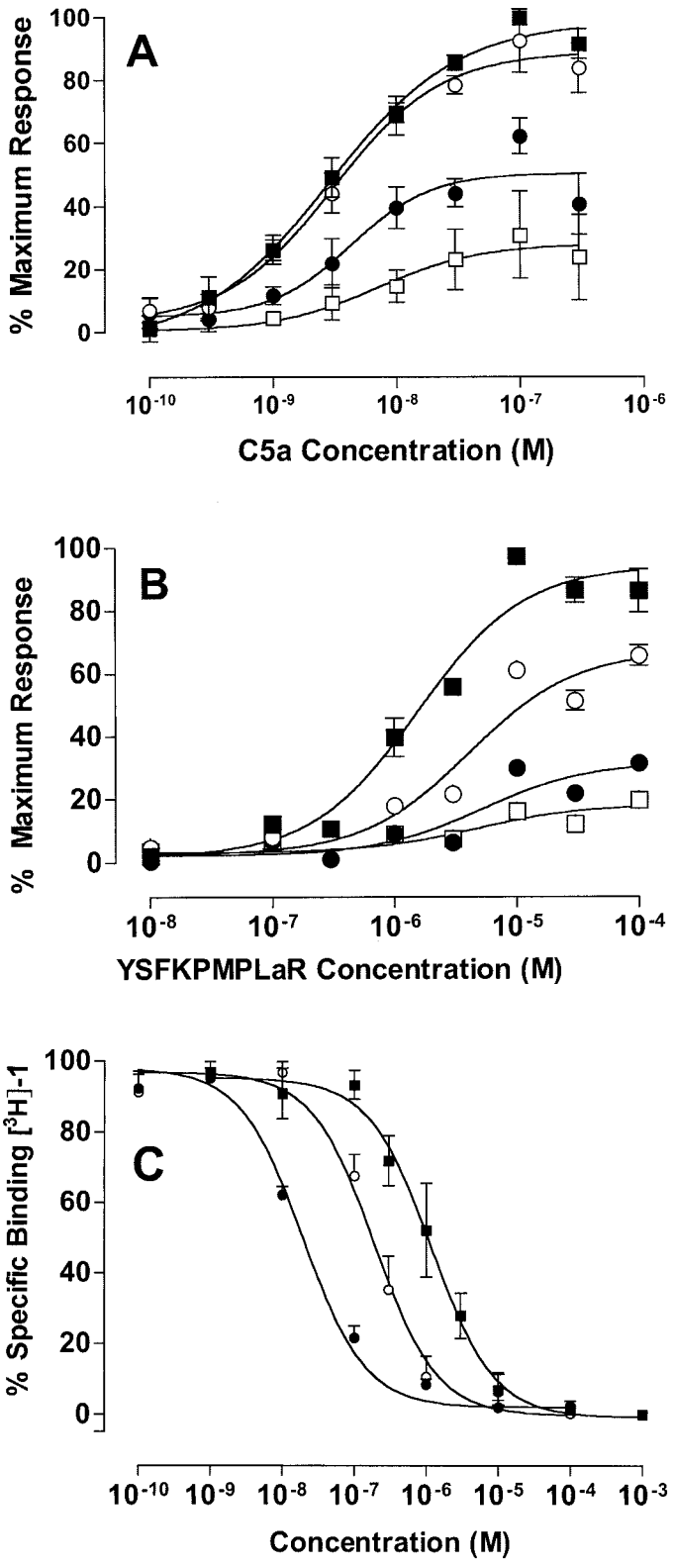

Fig. 2. (A&B) Antagonist potency in vitro. Myeloperoxidase release from human PMNLs incubated with C5a (A) or agonist YSFKPMPLaR (B) in the presence of antagonist **1** at 0 nM (■), 10 nM (○), 30 nM (●), and 100 nM (□). Data expressed as percentage maximum C5a or agonist response (mean ± S.E., n = 3–6). C, ligand competition for C5aR. Competitive binding (mean percentage of specific binding ± S.E., n = 3–4) for unlabeled **1** (●), MeFKPdChaWr (○), and YSFKPMPLAR (■) versus [^{3}H]labeled **1** for PMNLs.

constants for these residues, two χ-1 angle restraints (Phe and Trp) were obtained from 1D and ECOSY data with NOE intensities from a short mixing time NOESY. These five restraints were used in the structure calculations. Variable temperature data show low temperature coefficients $\Delta\delta$/T for Arg-δNH (2.7 ppb/K), Orn-δNH (1.8 ppb/K) and Arg αNH (2.7 ppb/K). In DMSO-d_6 containing 15% D_2O, both Trp and Arg αNHs underwent slower H/D exchange (56% and 62% residual signal intensities after 11 h) than other NHs (which exchanged in a few minutes), suggesting some protection from solvation as expected for H-bonded amide NHs. TOCSY spectra during the D_2O exchange experiment also support some H-bonding for the Orn δNH. In combination these three observations support the existence of some transannular H-bonding in a small population of solution structures that constitute **1**.

Structure Calculation. The 20 lowest energy structures (ΔE <1.3 kJ/mol) shown in Fig. 3 were calculated (Brünger, 1992) from 129 NOE restraints and 5 dihedral angles. The χ-1 restraints tightened the structure, with Phe and Trp rings being well defined. The root-mean-square deviation for all backbone atoms of the cycle was 0.27 Å. The Arg αNH and Orn δNH are directed to the interior of the saddle-shaped macrocycle. The Arg αNH was not within H-bonding distance to the nearest CO of Pro (CO. . . N 4.2Å), nor to CO of D-Cha (CO. . . N 4.4Å) as reported (Finch et al., 1999). Analysis with Promotif suggests the lowest energy structure is a type IV β-turn, but the protection from solvent of Trp and Arg αNHs suggests some type I-like β-turn in water.

NMR-derived solution structure calculations for small cyclic peptides are always compromised by the tendency of software packages to select out lowest energy structures from conformational ensembles (Nikiforovich et al., 2000). NMR parameters are time- and ensemble-averaged quantities, so NOE and J-couplings correspond to population-weighted averaged values, and single conformations calculated from such data may not reflect the overall structure, unless that conformation is highly populated. In the case of **1**, a very weak NOE between the acetyl methyl and the ArgαNH biases the structure (Fig. 3A) so that AcPhe moves beneath the plane of the macrocycle. A structure calculation without this NOE resulted in a flatter macrocycle with the Ac-Phe directed further away (Fig. 3B). We attribute the NOE to a small population of conformers where the AcPhe is located within NOE distance of the ArgαNH. This does not affect the Cα-Cβvectors of Pro, dCha, Trp, and Arg but does reorient the Phe side chain. The cyclic backbone structure identified here for **1** shows reasonably well how it acts as a scaffold in

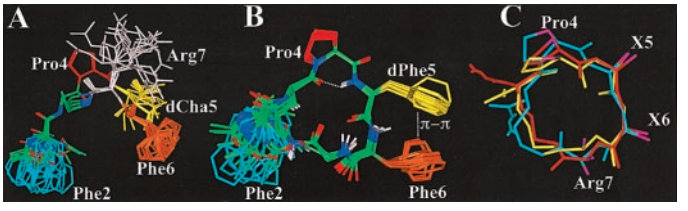

Fig. 3. Solution structure of **1**. A, average backbone structures with (yellow) and without (blue) a weak NOE (Ac→ArgαNH) constraint (AcPhe omitted). B, side view showing different locations for Ac-Phe substituent. C, overlay of 20 lowest energy structures in d_6-DMSO (Phe2, blue; Pro4, red; dCha5, yellow; Trp6, brown; Arg7, white) showing only the lowest energy conformer for cyclic backbone. Arg7 is directed away from dCha, Trp, and Phe.

projecting the side chains responsible for affinity (Phe, dCha, Trp, and Arg) and antagonism (Trp) into receptor space.

Structural Comparison of 1 with Acyclic Agonists/Antagonists

Small peptides derived from the C terminus of C5a typically show partial agonist activity in promoting enzyme release from human PMNLs (Luly et al., 1993; Konteatis et al., 1994, 1997; Siciliano et al., 1994; Sanderson et al., 1995; Finch et al., 1997). Decapeptide YSFKPMPLaR is one of the most potent examples of a full agonist, with an apparent receptor affinity for human PMNLs of 5 μM (Finch et al., 1997). Before our work, the only known C5aR antagonist was a hexapeptide analog of the C terminus of C5a, MeFKPdChaWr (Konteatis et al., 1994). We now show (Fig. 4A) for the first time that the NMR-derived solution structures of antagonist MeFKPdChaWr (Wong et al., 1998) and the small agonist peptide YSFKPMPLaR (Vogen et al., 1999) share a common 'turn' conformation (Fig. 4A) that is structurally mimicked by cyclic antagonist **1** (Fig. 4A). When this work was originally conducted, the C terminus of hC5a had been reported to be unstructured (Zuiderweg et al., 1989), but a more recent solution structure (Zhang et al., 1997) defined an elongated helical turn for residues $C5a_{70-74}$ (Fig. 4B), a turn that is mimicked by the cyclic component of **1** (Fig. 4C). This latter comparison suggests the possibility that the C terminus of C5a might bind to its receptor as a turn motif, as seems to be true for many peptide ligands for GPCRs.

Structure-Activity Relationships

To probe features of **1** responsible for receptor affinity and antagonism, a series of analogs were constructed from a cyclic scaffold (Fig. 5) with variable substituents. Effects of structure on receptor binding and antagonist potency (Fig. 6) can be interpreted from Tables 1–4, which show mainly single substitutions at positions A-F (Fig. 5). All compounds were devoid of agonist activity at 10^{-10} to 10^{-4} M.

Position A. Substitution of Ac in AcF-[OPdChaWR]. Analogs **2–8** (Table 1), incorporating alkyl, aryl, benzoyl, and tosyl substitutions for acetyl at position A of AcF-[OPdChaWR], had comparable affinity and antagonist potency to **1** for PMNL C5aRs. Thus, the acetyl group can be replaced with a wide range of groups of variable size, hydrophobicity and hydrophilicity without substantially reducing receptor affinity or antagonist activity. Loss of the substituent altogether from position A still produces comparable receptor affinity (Finch et al., 1999). This position could therefore be modified to vary solubility, pharmacokinetic parameters, or to attach fluorescent or radiotracer labels.

Position B. Substitution of Phe in AcF-[OPdChaWR]. The importance of the interaction between Phe and the receptor was examined through substitutions that varied spatial and stereochemical constraints at position B (Table 1). Removal of the aromatic side chain (**9**) significantly lowered receptor affinity (97-fold), demonstrating the importance of this component. dPhe (**10**) at this position produced a 75-fold reduction in receptor affinity, whereas phenylglycine (**11**) slightly lowered receptor affinity and antagonist potency. Shifting the aromatic ring further from the backbone (homophenylalanine, **12**) reduced affinity and antagonist potency by ~20 fold. Substitution of the aromatic ring by fluorine at *ortho*- or *meta*- positions (**13–14**) did not affect affinity and antagonist potency, but an H-bond donor (tyrosine, **15**) reduced receptor affinity by ~20 fold. The Phe side chain is thus important for ligand binding and interacts stereospecifically with the receptor via the L-enantiomer. Figure 7A

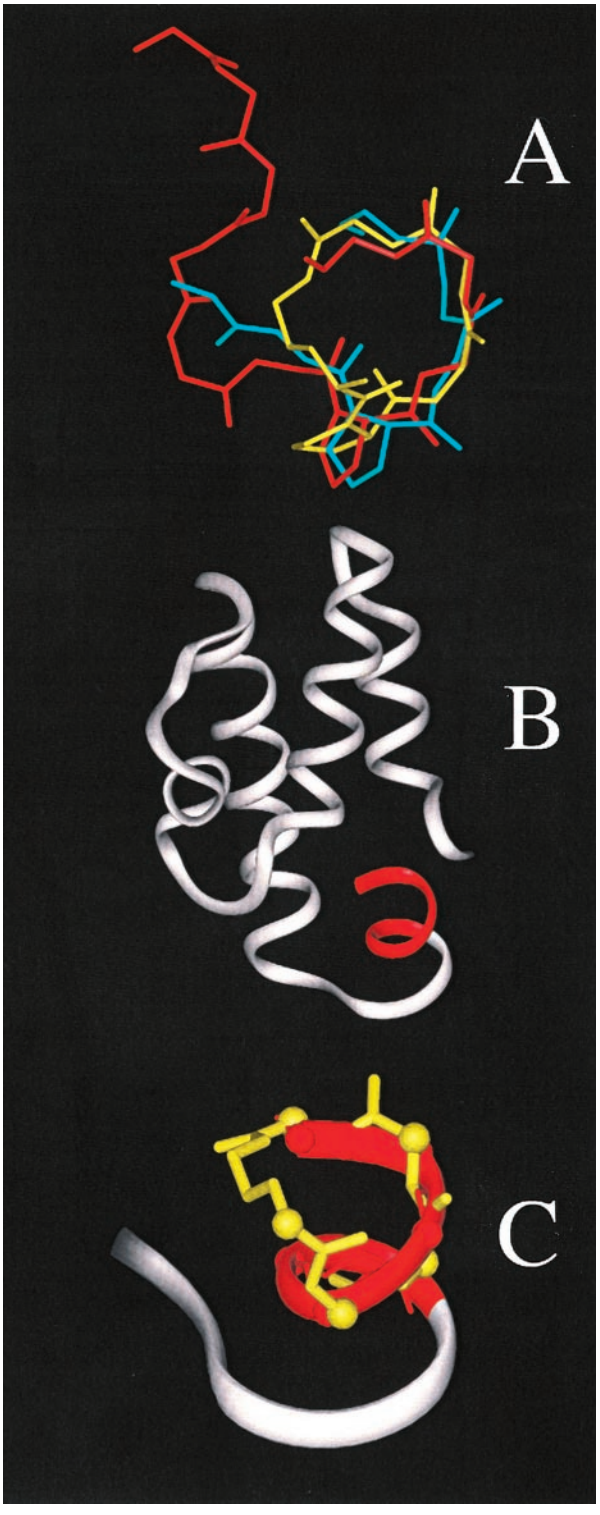

Fig. 4. Structural comparison of **1**, acyclic peptide agonist/antagonist, and C5a. Superimposed average solution structures derived from NMR spectroscopy for **1** (yellow) superimposed on agonist YSFKPMPLaR (red) (**38**) and antagonist MeFKPdChaWr (light blue) (**41**) (A); C5a (white with C-terminal residues 64–74 in red) (**29**) (B); **1** (yellow) superimposed on C-terminal residues 64–74 (red) showing balls for Cα atoms of each (C).

shows the relationship between receptor affinity and calculated steric volume for each side chain with L-stereochemistry; the steric fit of the side chain to receptor space is optimal for side chain volumes ~400 to 600 Å^3 because they showed highest affinity.

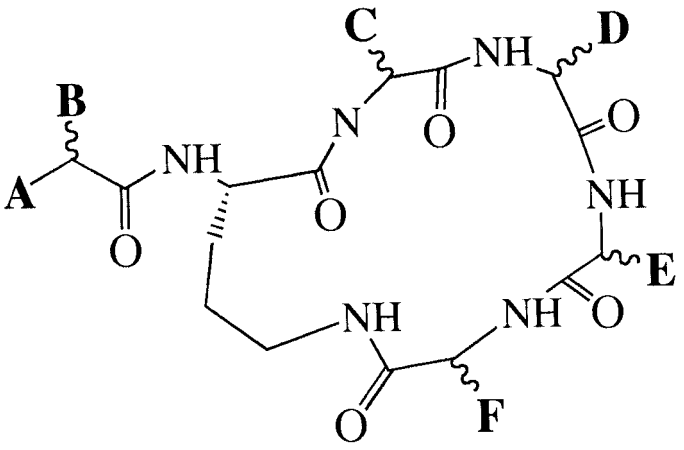

Fig. 5. Scaffold of C5a receptor antagonist cyclic peptides. Positions A-F were systematically varied in Tables 1–4.

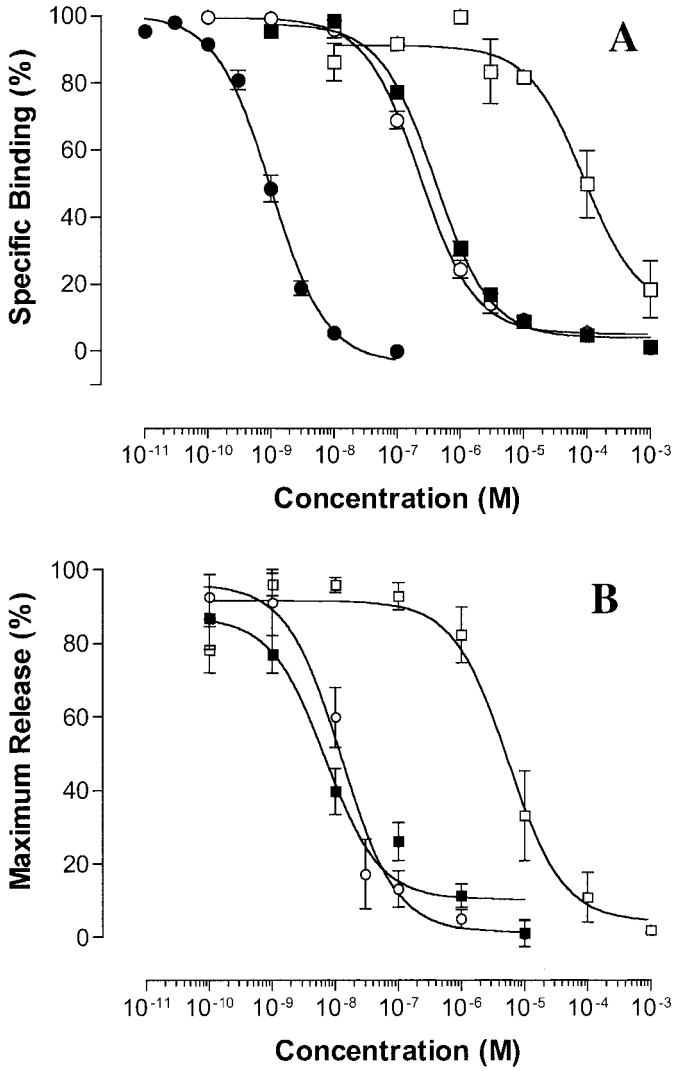

Fig. 6. Receptor affinity and antagonist potency. Inhibition by C5a (●), **1** (■), **18** (○), and **38** (□) of binding of ^{125}I-C5a to human PMNLs (A) and C5a-induced myeloperoxidase release from human PMNLs (B). Each point represents the mean ± S.E.M.

Positions A and B. Exocyclic substituents on AcF-[OPdChaWR]. Three analogs (**16**-**18**) simultaneously varied substituents at positions A and B on the cyclic scaffold (Table 1). Complete removal of the acetylated Phe (**16**), leaving only the cyclic component, diminished receptor affinity to undetectable levels. Attaching a cinnamoyl substitutent (**17**) to the macrocycle reduced (26-fold) receptor affinity, but hydrocinnamyl (**18**) did not alter C5aR affinity or antagonist potency. The negligible affinity of the cyclic scaffold [OPdChaWR] reveals how important the exocyclic component is for high affinity with C5aR. Because the substituent at position A is not crucial for binding, the Phe side chain contributes substantially to receptor affinity. Flexibility in the exocyclic appendage is important, the *trans* double bond of the cinnamoyl group has low affinity for the receptor, whereas the more flexible saturated hydrocinnamoyl appendage has affinity and potency comparable with **1**.

Position C. Substitution of Pro in AcF-[OPdChaWR]. Replacing proline in **1** by bulkier amino acids like Phe (**20**) and Ile (**21**) substantially reduced (6 and 8-fold, respectively) affinity for the cellular receptor (Table 2), but smaller Val (**19**), hydroxyproline (**22**), or δ-*N*-methyl-Orn (**24**) substituents had little effect on receptor affinity. The negligible effects of these smaller substituents indicate that they are merely filling receptor space without making important H-bonding or other intramolecular interactions. 4-*cis*-Thioproline (**23**, 75.5 μM) displayed a significant loss in binding affinity, whereas 4-*trans*-hydroxyproline (**22**, 0.45 μM) retained comparable affinity compared with **1**. These are of similar size and differ only in the stereochemistry, suggesting a steric fit to the receptor. Molecular replacements that did not possess the structural constraints and turn-inducing properties of Pro were not accommodated at this site. Figure 7B shows the relationship between receptor affinity and calculated steric volume for residues with L-stereochemistry at position C. An optimal minimum volume is not clear from this graph, although side chains >300 Å^3 cause a decrease in receptor affinity, presumably because receptor space is relatively limited for this position. The outlying point (β-thioproline) suggests that steric volume alone determines not only affinity but also how the steric bulk is oriented.

Position D. Substitution of D-Cha in AcF-[OPdChaWR]. D-Stereochemistry is crucial at this position for receptor affinity (Table 2), replacement of D-Cha by L-Cha results in IC_{50} 144 μM for receptor affinity (data not shown). Substitution of dCha with smaller aliphatic amino acids like D-norleucine (**29**), glycine (**25**), D-alanine (**26**), D-valine (**27**), and D-leucine (**28**) produced analogs with reduced receptor affinity (Table 2). Replacing cyclohexyl with an aromatic ring (**30**) or locating the cyclohexyl further from the scaffold (**32**) did not affect receptor affinity or antagonist potency. *N*-Methylation of phenylalanine (**31**) resulted in a 2000-fold loss in affinity for the C5aR. Tyr (**33**) at this position caused a 6-fold reduction in C5aR affinity, whereas incorporation of the positively charged arginine (**34**) eliminated binding up to 100 μM. Inclusion of a larger bicyclic residue (**36**), aminoindancarboxylic acid (**37**) or Trp (**35**) produced 24×, 60×, and 84× reduction in affinity. Antagonist potency for **26**, **30**, **32**, **33**, and **36** correlated with receptor affinity (Table 2), the

antagonist potencies of **30** and **32** were not significantly different from **1** (Table 2).

Figure 7C shows a parabolic relationship between receptor affinity and calculated steric volume of side chains, with one exception (D-homocyclohexylalanine). Because compounds with a larger or smaller side chains have lower affinity, the size/volume of this substitutent must be very important for receptor affinity. Removal of the dCha side chain dramatically reduces receptor affinity (**25**), neutral or charged polar side chains are contraindicated, whereas larger bicyclic substituents are not accommodated. A hydrophobic side chain extending at least two carbons from the α-carbon seems necessary for receptor affinity and antagonism. The dPhe substituent retains the affinity and activity of **1** but, given that other aliphatic groups can achieve this, it seems likely that this is caused by a hydrophobic interaction with the receptor rather than the π-stacking properties of this group. The dramatic loss in receptor affinity when the αNH at this position on the backbone is methylated (**31**) suggests a critical role for this group in forming either an intramolecular or a receptor-specific hydrogen-bonded interaction.

Position E. Substitution of Trp in AcF-[OPdChaWR]. Limitations in the size and orientation of the Trp replacement and the importance of the indole nitrogen of Trp were

TABLE 1
Structure-activity relationships at positions A and B of a C5a antagonist peptide

		Receptor Affinity			Antagonist Activity		
No.	Peptide	*n*	−log IC_{50} ± S.E.	IC_{50}[a]	*n*	−log IC_{50} ± SE	IC_{50}[b]
				μM			*nM*
1	Ac-F-[OPdChaWR]	22	6.43 ± 0.07	0.38	16	7.58 ± 0.06	26
2	Mes-F-[OPdChaWR]	3	6.32 ± 0.03	0.47	3	7.47 ± 0.13	34
3	Tos-F-[OPdChaWR]	3	6.01 ± 0.04	0.96	4	6.54 ± 0.15	291
4	Suc-F-[OPdChaWR]	3	6.35 ± 0.08	0.45	3	7.64 ± 0.17	23
5	MeSuc-F-[OPdChaWR]	3	6.07 ± 0.07	0.84	3	7.42 ± 0.07	38
6	Ahx-F-[OPdChaWR]	3	6.60 ± 0.06	0.25	3	7.21 ± 0.07	62
7	Bn-F-[OPdChaWR]	3	5.98 ± 0.08	1.10		N.D.	
8	Iso-F-[OPdChaWR]	3	6.07 ± 0.05	0.84		N.D.	
9	Ac-G-[OPdChaWR]	4	4.43 ± 0.11*	36.8		N.D.	
10	Ac-f-[OPdChaWR]	3	4.54 ± 0.12*	28.7		N.D.	
11	Ac-Phg-[OPdChaWR]	3	6.12 ± 0.05	0.76	3	6.82 ± 0.24	151
12	Ac-hPhe-[OPdChaWR]	3	5.17 ± 0.15*	6.8	2	6.32 ± 0.12*	480
13	Ac-(o-fl)F-[OPdChaWR]	3	6.28 ± 0.07	0.52	3	7.42 ± 0.11	38
14	Ac-(m-fl)F-[OPdChaWR]	2	6.36 ± 0.12	0.44		N.D.	
15	Ac-Y-[OPdChaWR]	2	5.05 ± 0.02*	8.9		N.D.	
16	H-[OPdChaWR]		Φ			N.D.	
17	Cin-[OPdChaWR]	3	5.00 ± 0.01*	9.90		N.D.	
18	HCin-[OPdChaWR]	3	6.65 ± 0.06	0.22	3	7.51 ± 0.12	31

[a] Concentration causing 50% inhibition of maximum binding of ^{125}I-C5a to intact PMNLs.
[b] Concentration causing 50% inhibition of myeloperoxidase release from PMNLs induced by 100 nM C5a.
Mes, mesyl; Tos, tosyl; Suc, succinyl; MeSuc, methyl succinyl; Ahx, aminohexanoyl; Bn, benzoyl; Iso, isovaleroyl; Phg, phenylglycine; hPhe, homophenylalanine; (o-fl)F, ortho-fluoro phenylalanine; (m-fl)F, meta-fluoro phenylalanine; Cin, cinnamoyl, Hcin, hydrocinnamoyl; N.D., not determined; *n*, number of experiments; *, significant at $P \leq 0.05$ difference from 1; Φ, no C5aR affinity up to 1 mM.

TABLE 2
Structure-activity relationships at positions C and D of C5a antagonist peptide

		Receptor Affinity			Antagonist Activity		
No.	Peptide	*n*	−log IC_{50} ± S.E.	IC_{50}[a]	*n*	−log IC_{50} ± SE	IC_{50}[b]
				μM			*nM*
19	AcF-[OVdChaWR]	2	6.08 ± 0.05	0.84		N.D.	
20	AcF-[OFdChaWR]	3	5.61 ± 0.0.7	2.43		N.D.	
21	AcF-[OIdChaWR]	3	5.53 ± 0.12*	2.94		N.D.	
22	AcF-[OHypdChaWR]	3	6.57 ± 0.20	0.27		N.D.	
23	AcF-[OThpdChaWR]	2	4.41 ± 0.20*	39		N.D.	
24	AcF-[(δ-N-Me)OPdChaWR]	3	6.45 ± 0.07	0.35	3	7.45 ± 0.03	35
25	AcF-[OPGWR]	3	2.97 ± 0.24*	1082		N.D.	
26	AcF-[OPdAlaWR]	3	3.84 ± 0.12*	145	3	4.43 ± 0.07*	3700
27	AcF-[OPdValWR]	3	4.89 ± 0.22*	13.0		N.D.	
28	AcF-[OPdLeuWR]	3	5.95 ± 0.04	1.13		N.D.	
29	AcF-[OPdNleWR]	3	6.27 ± 0.14	0.53		N.D.	
30	AcF-[OPdPheWR]	5	6.34 ± 0.12	0.46	3	7.65 ± 0.18	22
31	AcF-[OP(N-Me)fWR]	3	3.14 ± 0.83*	721		N.D.	
32	AcF-[OPdhChaWR]	3	6.41 ± 0.12	0.39	3	7.39 ± 0.1	41
33	AcF-[OPdTyrWR]	3	5.64 ± 0.17	2.2	3	6.53 ± 0.31	300
34	AcF-[OPdArgWR]	3		>100		N.D.	
35	AcF-[OPdTrpWR]	2	4.50 ± 0.15*	32		N.D.	
36	AcF-[OPdTicWR]	3	5.04 ± 0.07*	9.2	2	4.78 ± 0.22*	1665
37	AcF-[OPdAicWR]	3	4.64 ± 0.39*	22.7		N.D.	

[a] Concentration causing 50% inhibition of maximum binding of ^{125}I-C5a to intact PMNLs.
[b] Concentration causing 50% inhibition of myeloperoxidase release from PMNLs induced by 100 nM C5a.
Hyp, 4-trans-hydroxyproline; Thp, 4-cis-thioproline; (δ-N-Me)O, δ-N-methylated ornithine; (N-Me)f, *N*-methyl-D-phenylalanine; hCha, homocyclohexylalanine; Tic, tetrahydroisoquinoline; Aic, aminoindanecarboxylic acid; N.D., not determined; n, number of experiments; *, significant ($P \leq 0.05$) difference from 1; Φ, no C5aR affinity up to 1 mM.

investigated (Table 3). Smaller aliphatic residues Leu (**38**) and Cha (**39**) reduced receptor affinity 50× and 31×, respectively. Retaining the aromatic character of the indole moiety while reducing the size of the aromatic ring to an imidazole (**40**) resulted in a 62-fold loss in receptor affinity. In contrast, the smaller aromatic Phe (**41**) produced no significant change in receptor affinity, although extending the aromatic ring further from the cycle (**42**) caused a 30-fold reduction in affinity. *N*-Methylated Phe (**43**) significantly reduced affinity, as did substitution with dTrp (**44**). Incorporating benzothiazolealanine (**45**), which retains the size and aromaticity of the indole ring while exchanging sulfur for nitrogen, resulted in no change in receptor affinity. With the exception of 1-naphthyl (**46**), the incorporation of large bi- or tri-cyclic groups (**47–49**) reduced affinity for the C5aR. Of the three high-affinity analogs, two (**41**, **46**) were more potent antagonists than the third (**45**).

Figure 7D shows the variation in C5aR affinity for compounds containing an L-residue at this position, with calculated steric volume of side chains. Volume was calculated by rotation of all rotatable bonds through all sterically accessible positions and therefore represents the maximal volume of all side-chain–accessible space. An unambiguous minimum is not clear from this graph, however it does demonstrate that any side chain that is >900 Å^3 or <400 Å^3 results in decreased receptor affinity. We attribute these limitations to the receptor space, into which the side chain fits, being too small to accommodate the ligand in the case of the large side chains or too large to be adequately filled in the case of the smaller side chains.

Position F. Substitution of Arg in AcF-[OPdChaWR]. Three analogs (**50-52**; Table 3) report on the importance of size and charge of the Arg side chain for affinity. Removing the positive charge through substitution with citrulline (**50**) caused a 15-fold reduction in receptor affinity; moving the Arg side chain one carbon further from the cycle (**51**) decreased affinity 3-fold, and a Lys substitution (**52**) produced a 63-fold loss in receptor affinity. A terminal Arg in C5a has been shown to be critical for its activity (DeMartino et al., 1995) and is present in all C5a peptide analogs. Interaction between C5aR and the positively charged Arg side chain also contributes significantly to affinity of these cyclic antagonists. A low-affinity interaction can still occur when the positive charge is removed, because the urea moiety in citrulline confers high affinity.

Positions D to F of AcF-[OPdChaWR]. Based on the results for analogs with single substitutions at either dCha, Trp, or Arg (positions D-F), a number of compounds featuring

TABLE 3
Structure-activity relationships at position E or F of C5a antagonist peptides

		Receptor Affinity			Antagonist Activity		
No.	Peptide	*n*	−log IC_{50} ± S.E.	IC_{50}[a]	*n*	−log IC_{50} ± SE	IC_{50}[b]
				μM			*nM*
38	AcF-[OPdChaLR]	3	4.72 ± 0.13*	18.9	3	5.52 ± 0.43*	3000
39	AcF-[OPdChaChaR]	3	4.92 ± 0.17*	11.9	3	5.34 ± 0.02*	4500
40	AcF-[OPdChaHR]	3	4.63 ± 0.10*	23.5		N.D.	
41	AcF-[OPdChaFR]	3	6.61 ± 0.15	0.25	3	7.49 ± 0.07	32
42	AcF-[OPdChahFR]	3	4.93 ± 0.24*	11.7		N.D.	
43	AcF-[OPdCha(N-Me)FR]	3	4.47 ± 0.11*	27.2		N.D.	
44	AcF-[OPdChawR]	3	4.52 ± 0.14*	30.4		N.D.	
45	AcF-[OPdChaBtaR]	3	6.55 ± 0.28	0.28	3	6.76 ± 0.27	172
46	AcF-[OPdCha1NalR]	3	6.15 ± 0.01	0.71	3	7.33 ± 0.22	47
47	AcF-[OPdCha2NalR]	3	5.80 ± 0.06	15.8		N.D.	
48	AcF-[OPdChaTicR]	3	5.43 ± 0.39*	3.7	2	4.95 ± 0.19*	1130
49	AcF-[OPdChaFlaR]	3	4.54 ± 0.20*	28.9	3	6.10 ± 0.09*	800
50	AcF-[OPdChaWCit]	3	5.22 ± 0.06*	6.0		N.D.	
51	AcF-[OPdChaWhArg]	3	5.87 ± 0.06	1.4		N.D.	
52	AcF-[OPdChaWK]	3	4.62 ± 0.05*	24.1		N.D.	

[a] Concentration causing 50% inhibition of maximum binding of ^{125}I-C5a to intact PMNLs.
[b] Concentration causing 50% inhibition of myeloperoxidase release from PMNLs induced by 100 nM C5a.
hPhe, homophenylalanine; (N-Me)F, *N*-methyl phenylalanine; Bta, benzothiazolealanine; 1Nal, 1-Napthylalanine; 2-Nal, 2-napthylalanine; Tic, tetrahydroisoquinoline; Fla, fluorenylalanine; Cit, citrulline; hArg, homoarginine; N.D., not determined; n, number of experiments; *, significant ($P \leq 0.05$) difference from 1; Φ, no C5aR affinity up to 1 mM.

TABLE 4
Structure-activity relationships at positions D and E or E and F of C5a antagonist peptides in combination

		Receptor Affinity			Antagonist Activity		
No.	Peptide	*n*	−log IC_{50} ± S.E.	IC_{50}[a]	*n*	−log IC_{50} ± SE	IC_{50}[b]
				μM			*nM*
53	AcF-[OPfFR]	5	5.29 ± 0.22*	5.2	3	5.28 ± 0.10*	5210
54	AcF-[OPf1NalR]	3	5.51 ± 0.04*	3.1		N.D.	
55	AcF-[OPfYR]	3	4.16 ± 0.13*	69.2		N.D.	
56	AcF-[OPdChaF(pCl)F]	3	5.50 ± 0.09*	3.2		N.D.	
57	AcF-[OPdChaF(pNH_2)F]	3	5.46 ± 0.10*	3.5		N.D.	
58	AcF-[OPdChaFhF]	3	5.17 ± 0.15*	6.8		N.D.	
59	AcF-[OPdArgFR]	3		>1 mM		N.D.	
60	AcF-[OPGmbTyrR]	3	6.03 ± 0.08	0.93	2	6.17 ± 0.09*	679

[a] Concentration causing 50% inhibition of maximum binding of ^{125}I-C5a to intact PMNLs.
[b] Concentration causing 50% inhibition of myeloperoxidase release from PMNLs induced by 100 nM C5a.
(pCl)F, *para*-chlorophenylalanine; (pNH_2)F, *para*-aminophenylalanine; hPhe, homophenylalanine; mbTyr, metabenzyltyrosine; N.D., not determined; n, number of experiments; *, significant ($P \leq 0.05$) difference from 1; Φ, no C5aR affinity up to 1 mM.

double changes were synthesized (Table 4). Three analogs incorporated dPhe at position D and either Phe (**53**), 1-napthylalanine (**54**), or Tyr (**55**) at position E. Analogs **56–58** showed significantly reduced binding affinity. A fourth compound incorporating dArg (**59**) at position D and Phe at position E had no detectable affinity up to 1 mM. Complete removal of the dCha sidechain via a Gly substitution coupled with incorporation of a *meta*-benzyl tyrosine at the Trp position (**60**) did not have a significant effect on receptor affinity. Analogs **53** and **60** were less potent antagonists.

Attempts to simultaneously change dCha and Trp residues to the most favorable residues identified from above led to reduced affinity and activity. Either there is a complex spatial interaction between the groups at these sites or the receptor responds cooperatively to simultaneous changes on the ligand. The receptor affinity and antagonist activity of the double Phe substitution does not correlate with the other AcF-[OPdChaWR] analogs. The disproportional loss in activity seen with these substitutions underlines the complexity of cooperative protein-ligand interactions. Optimal binding at one location can become unfavorable if changes are made elsewhere because of the interactions that are induced after compound binding. Ligand-protein interactions are not rigid 'lock and key' contacts that can be readily optimized. Both the receptor and the antagonist are flexible and changes at one site can have unintended and unpredictable effects at another site.

Solution Structures of 41 and 53

We determined solution structures of active (**41**) and inactive (**53**) compounds to investigate whether cyclic backbone shape is altered by side-chain variation. This is important because side-chain bulk can either influence ligand fit to the receptor directly or indirectly, via changes to macrocycle shape.

Structure of 41 (Ac-Phe[Orn-Pro-dCha-Phe-Arg]). ^{1}H NMR spectra for **41** in DMSO-d_6 were similar to those for **1** with seven well resolved amide NH resonances. Indicators of local structure were the $^3J_{H\alpha,NH}$ coupling constants for Phe2 (8.5 Hz), D-Cha5 (4.6 Hz), and Arg7 (8.3 Hz). Like **1**, **41** shows low temperature coefficients ($\delta\Delta$/K) for Arg αNH (2.3 ppb/K), Orn δNH (2.4 ppb/K), and Arg δNH (2.7 ppb/K). Stereospecific assignments of β-protons and χ-1 dihedral restraints for Phe2 and Phe6 were determined as for **1**. The solution structure of **41** was calculated from 79 NOE restraints and 5 dihedral angle restraints to produce 20 convergent lowest energy structures (ΔE <0.3 kJ/mol) shown in Fig. 8A. The root-mean-square deviation over all backbone atoms of the cycle was 0.12 Å. The Ac-Phe portion of the molecule is less defined than in **1**, because of the difficulty in unambiguously assigning NOEs from aromatic residues to Phe2 or Phe6. The Pro Cα. . . Arg Cαdistance (5.7 Å) was shorter than in **1** (6.9Å), and this may reflect a higher population of Type II′ β-turn conformers.

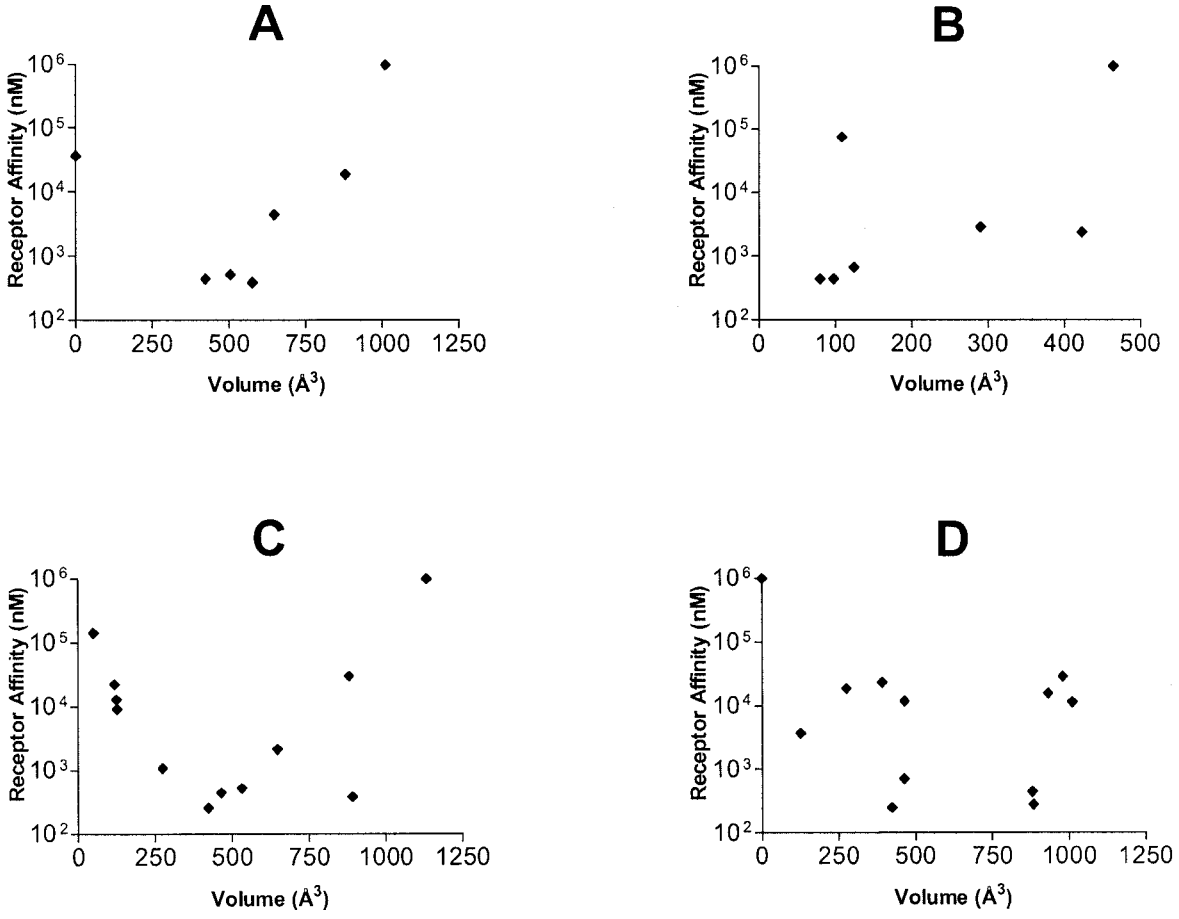

Fig. 7. Volume-Affinity Relationships. Calculated steric volume of the side chain versus measured affinity for PMNLs of analogs of **1** with replacements for Phe (**10–17**) (A); Pro (**19–24**) (B); D-Cha (**25-37**) (C); and Trp (**38-49**) (D).

Structure of 53 (Ac-Phe[Orn-Pro-dPhe-Phe-Arg]). In contrast to **1** and **41**, $^3J_{H\alpha,NH}$ coupling constant for D-Phe5 (6.5 Hz) was not indicative of structure, whereas Phe2 (8.3 Hz) and Arg7 (8.3 Hz) were similarly high and used to derive two ϕ dihedral angle restraints. Variable-temperature NMR experiments indicated low-temperature coefficients for Arg αNH (1.7 ppb/K), D-Phe5 (2.4 ppb/K), and Arg δNH (2.7 ppb/K). All three possible sets of stereospecific Hβ-assignments (Phe2, dPhe5, Phe6 AMX spin systems) and three χ-1 dihedral restraints could be extracted from 1D ^{1}H and ECOSY data. NMR structure calculations based on 71 NOE restraints and the 5 dihedral restraints yielded a highly converged family of structures (Fig. 8B) with cycle backbone pairwise root-mean-square deviation = 0.15 Å. The 20 lowest energy structures (Fig. 8B) describe an inverse γ-turn about Orn-Pro-D-Phe and suggest a π-π interaction between D-Phe5 and Phe6. The D-Phe5 αNH does not exchange rapidly with D_2O; Arg and Trp αNHs were also somewhat slow to exchange.

Comparision of Structures. Fig. 8C shows a superimposition of the average calculated structures for **1**, **41,** and **53** using all macrocycle backbone heavy atoms. The three structures show remarkable similarity in the position of their cyclic Cα-Cβ side chain vectors, suggesting that subtle alterations to the cyclic backbone may not dramatically disrupt the projections of the side chains. Thus, the steric bulk of side chains will probably directly determine affinity and antagonism.

Discussion

In contrast to reported peptide analogs of the C terminus of C5a, cyclic antagonist **1** is a potent antagonist of the C5aR on human PMNLs, and it is devoid of agonist activity, as monitored in sensitive assays for chemotaxis and polarization (Haynes et al., 2000). It is also highly receptor selective, failing even at 100 μM concentrations to antagonize myeloperoxidase release from PMNLs stimulated with fMet-Leu-Phe, leukotriene B_4, platelet-activating factor (Finch et al., 1999), C3a, or IL-8 (N. Paczkowski, K. Wadi, and S. M. Taylor, unpublished data). Unlike linear peptides and complement-targeting proteins, cyclic antagonist **1** is chemically stable to peptidase degradation in blood and gastric fluids (data not shown) and is both small enough and sufficiently lipophilic to be orally active at $\leq$1 mg/kg/day in vivo (Woodruff et al., 2002). We have found that **1** has potent and efficacious anti-inflammatory activity in short- and long-term rat models of sepsis (Short et al., 1999; Huber-Lang et al., 2002), reverse passive Arthus (Strachan et al., 2000) dermal inflammation (Strachan et al., 2001), arthritis (Woodruff et al., 2002), gastrointestinal and renal ischemia-reperfusion injury (Arumugam et al., 2002, 2003), and colitis (Woodruff et al., 2003). This anti-inflammatory activity is partly related to indirect inhibition of the release of proinflammatory cytokines (e.g., TNFα, IL-6) from PMNLs, monocytes, and other immune cells that we have directly monitored (Haynes et al., 2000; Strachan et al., 2000; Arumugam et al., 2002).

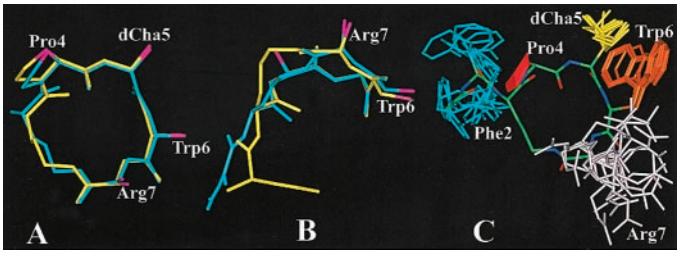

Fig. 8. Superimposition of Structures. Overlay of 20 lowest energy structures of **41** (A) and **53** (B) (Phe2, blue; Pro4, red; dCha5, yellow; Phe6, brown; Arg7, white but not shown for clarity in **53**). Putative π-π interaction and inverse γ-turn defining H-bond around Pro4 are shown for **53**. C, overlay of averaged structures for cyclic backbones of **1** (red), **41** (yellow), and **53** (blue, β-carbons for residues 4–7 in cyan).

In the absence of detailed structural knowledge of the transmembrane protein C5aR and its active site, structure-activity relationships for ligands that bind to the human C5a receptor can provide valuable information for defining the agonist/antagonist binding site and for the development of potent C5aR agonists and antagonists. We reported herein the refined solution structure (Fig. 3) of our prototype cyclic antagonist AcF[OPdChaWR] (**1**) consisting of a cyclic scaffold that supports affinity-determining and antagonist-defining side chain moieties. Structural comparisons between cyclic antagonist **1**, the C terminus of C5a, and a small acyclic peptide agonist and antagonist (Fig. 4) suggest the importance of a common turn conformation for receptor binding. The turn shape in **1** is also displayed by cyclic analogs [e.g., **41** and others (M. J. Stoermer and D. P. Fairlie, unpublished results)]. Together with this structural similarity, competition between cyclic antagonist **1** and either C5a or acyclic peptide agonist or antagonists for the C5aR on whole PMNLs (Fig. 2) is consistent with a common bioactive shape for the antagonist, agonist and C terminus of C5a, and supports the same or a similar binding site on C5aR.

To understand the influence of each component of **1** on receptor affinity and antagonist potency, structure-activity relationships were investigated for 60 cyclic analogs of **1** evaluated against the C5aR on human PMNLs by radioligand binding for receptor affinity and by enzyme release for antagonist potency. Twenty compounds had receptor affinities $IC_{50} < 1$ μM. There was a positive general correlation between affinity and antagonism for the majority of analogs examined, allowing insights to size and shape limitations at each antagonist position. The solution structures for cyclic analogs of **1** [**41, 53,** and others not shown (M. J. Stoermer and D. P. Fairlie, unpublished results)] reveal a common cyclic backbone shape, supporting the idea that side chain variations directly affect ligand fit to the receptor rather than indirectly by altering macrocyclic shape. This is further supported by relationships between calculated steric volume of side chains and measured affinity for PMNLs (Fig. 7) that reveal optimal side chain bulk at each site on the cyclic antagonist scaffold. Whereas position A (Ac) can be varied widely without loss in potency, positions B (Phe), C (Pro), D (D-Cha), and F (Arg) are likely determinants of receptor affinity rather than antagonist potency per se, and position E (Trp) alone seems to mechanistically dictate whether the cyclic scaffold will be an antagonist or agonist. The latter observation is similar to what was learned from acyclic peptide ligands for C5a (Konteatis et al., 1994), except that side chains other than the indole ring of Trp (e.g., Phe) on the cyclic scaffold also produce potent antagonism herein and the Arg needs to have L- rather than the D-stereochemistry (Wong et al., 1998) preferred for acyclic antagonists. Inter-

estingly the NMR structure of **53** supports a similar cyclic scaffold to that in **1** but also suggests D-Phe. . . . L-Phe π-stacking interaction in DMSO-d6. In a hydrophobic receptor environment, this may interfere with ligand fitting associated with antagonism because compound **53** was not a potent antagonist.

The availability of potent and selective antagonists of the C5aR can help to establish the pathophysiology of C5a and to probe the selective pathological responses to this component of the complement network. C5a formation or action is inhibited in vivo by soluble recombinant complement receptor type I (sCR1) (Hill et al., 1992), C5 and C5a antibodies (Amsterdam et al., 1995; Wang et al., 1995), or recombinant C5a polypeptides (Pellas et al., 1998) but these large molecules have inherent limitations as drugs, including poor bioavailability, low metabolic stability, potential immunogenicity, and manufacturing costs. Here we reported a series of novel small molecules, derived from the solution structure of just a small portion of the bioactive surface of C5a, 20 of which are potent ($IC_{50} < 1$ μM) and selective antagonists of human C5aR. This class of cyclic compounds shows promising anti-inflammatory activity in vivo even when given orally, so structure-activity relationships reported herein serve to define a pharmacophore for potential development of C5aR-directed small molecule anti-inflammatory drugs. In conjunction with site-directed mutagenesis studies of the receptor, these data may help to better define the mechanism of agonism versus antagonism, enabling a better understanding of the origin and control of C5a-mediated disease pathology.

Rational drug design based on protein-protein interactions has often proven to be frustrating for medicinal chemists, particularly the development of small nonpeptidic antagonists of protein hormones and cytokines. Some important pathogenic factors, such as TNFα, can be controlled by antagonist drugs now in the clinic (e.g., Enbrel), but they are mainly protein-based therapies requiring parenteral administration. The immediate challenge is to understand surface protein-protein interactions in sufficient detail to enable the development of small orally active antagonists. The structure- and ligand-based approach demonstrated here for a G protein-coupled receptor, uses constrained cyclic molecules as intermediates in the development of nonpeptidic drugs. Such cyclic intermediates can provide valuable insight to the receptor-binding ligand structure and are sometimes suitable in their own right as orally active molecular probes for in vivo target validation, as in this case.

References

Abbas AK, Lichtman AH, and Pober JS (1997). The complement system, in *Cellular and Molecular Immunology*, pp 315–338, WB Saunders, Philadelphia.

Amsterdam EA, Stahl GL, Pan HL, Rendig SV, Fletcher MP, and Longhurst JC (1995) Limitation of reperfusion injury by a monoclonal antibody to C5a during myocardial infarction in pigs. *Am J Physiol* **268:**448–457.

Arumugam TV, Shiels IA, Strachan AJ, Abbenante G, Fairlie DP, and Taylor SM (2003) A small molecule C5a receptor antagonist protects kidneys from ischemia/reperfusion injury in rats. *Kidney Int* **63:**134–142.

Arumugam TV, Shiels IA, Woodruff TM, Reid RC, Fairlie DP, and Taylor SM (2002) Protective effect of a new C5a receptor antagonist against ischemia-reperfusion injury in the rat small intestine. *J Surg Res* **103:**260–267.

Barnum SR (2002) Complement in central nervous system inflammation. *Immunol Res* **26:**7–13.

Brünger AT (1992). *X-PLOR Manual Version 3.1.* Yale University, New Haven, CT.

DeMartino JA, Konteatis ZD, Siciliano SJ, Van RG, Underwood DJ, Fischer PA, and Springer MS (1995) Arginine 206 of the C5a receptor is critical for ligand recognition and receptor activation by C-terminal hexapeptide analogs. *J Biol Chem* **270:**15966–15969.

Drapeau G, Brochu S, Godin D, Levesque L, Rioux F, and Marceau F (1993) Synthetic C5a receptor agonists. Pharmacology, metabolism and in vivo cardiovascular and hematologic effects. *Biochem Pharmacol* **45:**1289–1299.

Ember JA, Jagels MA, and Hugli TE (1998). Characterization of complement anaphylatoxins and their biological responses, in *The Human Complement System in Health and Disease* (Volanakis JE, Frank MM eds) pp. 241–284, Marcel Dekker, New York.

Ember JA, Sanderson SD, Hugli TE, and Morgan EL (1994) Induction of interleukin-8 synthesis from monocytes by human C5a anaphylatoxin. *Am J Pathol* **144:**393–403.

Finch A, Vogen S, Sherman S, Kirnarsky L, Taylor S, and Sanderson S (1997) Biologically active conformer of the effector region of human C5a and modulatory effects of N-terminal receptor binding determinants on activity. *J Med Chem* **40:**877–884.

Finch AM, Wong AK, Paczkowski NJ, Wadi SK, Craik DJ, Fairlie DP, and Taylor SM (1999) Low-molecular-weight peptidic and cyclic antagonists of the receptor for the complement factor C5a. *J Med Chem* **42:**1965–1974.

Haynes DR, Harkin DG, Bignold LP, Hutchens MJ, Taylor SM, and Fairlie DP (2000) Inhibition of C5a-induced neutrophil chemotaxis and macrophage cytokine production in vitro by a new C5a receptor antagonist. *Biochem Pharmacol* **60:**729–733.

Hill J, Lindsay TF, Ortiz F, Yeh CG, Hechtman HB, and Moore FD Jr (1992) Soluble complement receptor type 1 ameliorates the local and remote organ injury after intestinal ischemia-reperfusion in the rat. *J Immunol* **149:**1723–1728.

Huber-Lang MS, Riedeman NC, Sarma JV, Younkin EM, McGuire SR, Laudes IJ, Lu KT, Guo RF, Neff TA, Padgaonkar VA, et al. (2002) Protection of innate immunity by C5aR antagonist in septic mice. *FASEB J* **16:**1567–1574.

Huber-Lang MS, Sarma JV, McGuire SR, Lu KT, Padgaonkar VA, Younkin EM, Guo RF, Weber CH, Zuiderweg ER, Zetoune FS, et al. (2003) Structure-function relationships of human C5a and C5aR. *J Immunol* **170:**6115–6124.

Kenakin TP (1997). *Pharmacologic Analysis of Drug-Receptor Interaction*. Lippincott-Raven, New York.

Kohl J (2001) Anaphylatoxins and infectious and non-infectious inflammatory diseases. *Mol Immunol* **38:**175–187.

Konteatis Z, Siciliano SJ, and Springer MS (1997) inventors, Merck & Co., Inc., assignee. Assay to identify human C5a antagonists and agonists U.S. patent 5,614,370. 1997 Mar 25.

Konteatis ZD, Siciliano SJ, Van Riper G, Molineaux CJ, Pandya S, Fischer P, Rosen H, Mumford RA, and Springer MS (1994) Development of C5a receptor antagonists. Differential loss of functional responses. *J Immunol* **153:**4200–4205.

Luly JR, Kawai M, and Wiedeman PE (1991), inventors, Abbott Laboratories, assignee. Terminally modified tri-, tetra- and pentapeptide anaphylatoxin receptor ligands. U.S. patent 5,190,922. 1991 Jun 4.

Nikiforovich GVK, Kover E, Zhang WJ, and Marshall GR (2000) Cyclopentapeptides as flexible conformational templates. *J Am Chem Soc* **122:**3262–3273.

Okusawa S, Yancey KB, van der Meer JW, Endres S, Lonnemann G, Hefter K, Frank MM, Burke JF, Dinarello CA, and Gelfand JA (1988) C5a stimulates secretion of tumor necrosis factor from human mononuclear cells in vitro. Comparison with secretion of interleukin 1 beta and interleukin 1 alpha. *J Exp Med* **168:**443–448.

Paczkowski NJ, Finch AM, Whitmore JB, Short AJ, Wong AK, Monk PN, Cain SA, Fairlie DP, and Taylor SM (1999) Pharmacological characterization of antagonists of the C5a receptor. *Br J Pharmacol* **128:**1461–1466.

Pellas TC, Boyar W, van Oostrum J, Wasvary J, Fryer LR, Pastor G, Sills M, Braunwalder A, Yarwood DR, Kramer R, et al. (1998) Novel C5a receptor antagonists regulate neutrophil functions in vitro and in vivo. *J Immunol* **160:**5616–5621.

Sanderson SD, Kirnarsky L, Sherman SA, Ember JA, Finch AM, and Taylor SM (1994) Decapeptide agonists of human C5a: the relationship between conformation and spasmogenic and platelet aggregatory activities. *J Med Chem* **37:**3171–3180.

Sanderson SD, Kirnarsky L, Sherman SA, Vogen SM, Prakash O, Ember JA, Finch AM, and Taylor SM (1995) Decapeptide agonists of human C5a: the relationship between conformation and neutrophil response. *J Med Chem* **38:**3669–3675.

Short A, Wong AK, Finch AM, Haaima G, Shiels IA, Fairlie DP, and Taylor SM (1999) Effects of a new C5a receptor antagonist on C5a- and endotoxin- induced neutropenia in the rat. *Br J Pharmacol* **126:**551–554.

Siciliano SJ, Rollins TE, DeMartino J, Konteatis Z, Malkowitz L, Van RG, Bondy S, Rosen H, and Springer MS (1994) Two-site binding of C5a by its receptor: an alternative binding paradigm for G protein-coupled receptors. *Proc Natl Acad Sci USA* **91:**1214–1218.

Strachan AJ, Shiels IA, Reid RC, Fairlie DP, and Taylor SM (2001) Inhibition of immune-complex mediated dermal inflammation in rats following either oral or topical administration of a small molecule C5a receptor antagonist. *Br J Pharmacol* **134:**1778–1786.

Strachan AJ, Woodruff TM, Haaima G, Fairlie DP, and Taylor SM (2000) A new small molecule C5a receptor antagonist inhibits the reverse-passive arthus reaction and endotoxic shock in rats. *J Immunol* **164:**6560–6565.

Vogen SM, Prakash O, Kirnarsky L, Sanderson SD, and Sherman SA (1999) Determination of structural elements related to the biological activities of a potent decapeptide agonist of human C5a anaphylatoxin. *J Pept Res* **54:**74–84.

Wang Y, Rollins SA, Madri JA, and Matis LA (1995) Anti-C5 monoclonal antibody therapy prevents collagen-induced arthritis and ameliorates established disease. *Proc Natl Acad Sci USA* **92:**8955–8959.

Wetsel RA (1995) Structure, function and cellular expression of complement anaphylatoxin receptors. *Curr Opin Immunol* **7:**48–53.

Wong AK, Finch AM, Pierens GK, Craik DJ, Taylor SM, and Fairlie DP (1998) Small molecular probes for G-protein-coupled C5a receptors: conformationally constrained antagonists derived from the C terminus of the human plasma protein C5a. *J Med Chem* **41:**3417–3425.

Woodruff TM, Arumugam TV, Shiels IA, Reid RC, Fairlie DP, and Taylor SM (2003) A potent human C5a receptor antagonist protects against disease pathology in a rat model of inflammatory bowel disease. *J Immunol* **171:**5514–5520.

Woodruff TM, Strachan AJ, Dryburgh N, Shiels IA, Reid RC, Fairlie DP, and Taylor SM (2002) Antiarthritic activity of an orally active C5a receptor antagonist against antigen-induced monarticular arthritis in the rat. *Arthritis Rheum* **46:**2476–2485.
Wuthrich K (1986). *NMR of Proteins and Nucleic Acids.* John Wiley and Sons, New York.
Zhang X, Boyar W, Toth MJ, Wennogle L, Gonnella NC (1997) Structural definition of the C5a C terminus by two-dimensional nuclear magnetic resonance spectroscopy. *Proteins* **28:**261–267.
Zuiderweg ER, Nettesheim DG, Mollison KW, and Carter GW (1989) Tertiary structure of human complement component C5a in solution from nuclear magnetic resonance data. *Biochemistry* **28:**172–185.
Zwirner J, Fayyazi A, and Gotze O (1999) Expression of the anaphylatoxin C5a receptor in non-myeloid cells. *Mol Immunol* **36:**877–884.

Address correspondence to: Professor David Fairlie, Institute for Molecular Bioscience, University of Queensland, St Lucia QLD 4072, Australia. E-mail: d.fairlie@imb.uq.edu.au